Development of a Three-Axis Active Vibration Isolator Using Zero-Power Control

Md. Emdadul Hoque, *Student Member, IEEE*, Masaya Takasaki, *Associate Member, IEEE*, Yuji Ishino, and Takeshi Mizuno, *Member, IEEE*

***Abstract*—This paper presents the development of an active 3-degree-of-freedom (DoF) vibration isolation system using zero-power magnetic suspension. The developed system is capable to suppress direct disturbances and isolate ground vibrations of the 3-DoF motions, associated with vertical translational and rotational modes. Two categories of control strategy for the actuators are proposed, i.e., local control and mode control. The latter method allows to overcome limitations of the poor performances for rotational modes exhibited by the former. A mathematical model of the system is derived and each DoF motion is treated separately for the control system. It is demonstrated analytically that the infinite stiffness to static direct disturbances can be generated and the resonance peak due to floor vibration can effectively be suppressed for the system. Moreover, the experiments have been carried out to measure the static and dynamic responses of the isolation table to direct disturbances, and transmissibility characteristic of the isolator from the floor. The results indicate good vibration isolation and attenuation performances, and show the efficacy of the developed isolator for industrialization.**

***Index Terms*—Active control, local control, mode control, vibration isolation, zero-power control.**

I. Introduction

MICROVIBRATION isolation has become a growing research field due to the demand of high-performance systems, and the advent of micro- and nanotechnology in various scientific and industrial fields such as semiconductor manufacturing, biomedical engineering, aerospace equipments, and high-precision measurements. These hi-tech research arenas need sophisticated systems that are isolated from microvibrations. For vibration isolation systems, it is inevitable to isolate ground vibrations in addition to the effect of direct disturbances. Direct disturbances to the system due to the change of load, use of electric motors and rotating devices on the table, and ground vibrations caused by other prime movers, and earthquake and movement of vehicles can, however, be the source of detrimental vibrations that may influence the effectiveness and accuracy of operations, and objective performances. Generally, the vibration-control research can be divided into two categories, i.e., active and passive control. For the former, external energy is necessary. On the other hand, no external energy is needed for the latter technique, and the vibration suppression is stable if the dynamic characteristic of the primary system are unchanged [1]. Suspension with higher stiffness can be used for suppressing the effect of direct disturbances while that of lower stiffness is suitable for isolating ground vibrations in case of conventional passive-type vibration isolation system [2]. So a tradeoff between the suspensions is necessary, which is the major drawback of this control technique.

Active control can overcome this setback and has been applied to several vibration isolation devices recently [3]–[7]. However, this technique requires external energy, in one hand, and high-performance sensors, such as servo-type accelerometers, on the other, and makes the system rather expensive.

To overcome these difficulties, the authors have proposed an active vibration-control technique using zero-power magnetic suspension [8]. This technique usually requires only eddy-current relative-displacement sensors that cost far less than servo-type accelerometers. Moreover, there is no steady power consumption in the system during stable operation [9], [10]. Since a zero-power system behaves as if it has a negative stiffness, infinite stiffness against disturbances on the isolation table can be achieved by combining it with a normal spring in series. It enables the system to have good characteristics both in reducing vibration transmitted from the ground and in suppressing direct disturbing force. It can be noted that negative stiffness can be realized by either passive or active techniques. Platus [11], [12] presented a passive-type vibration isolator by connecting a negative stiffness in parallel with a normal spring, and the isolator stiffness was made to approach zero for ground vibration isolation only. However, the effect of direct disturbance was not addressed in the research. Trumper and Sato [7] developed an isolator by connecting an active negative stiffness spring in parallel with a positive spring that achieved good vibration isolation performance and platform releveling by position and velocity control of the platform. Whereas, in that case, excessive heat was generated in the actuator caused by drive currents and power was consumed by the system. Therefore, the motivation of this paper is to develop a vibration isolator with low cost and to downsize the power consumption abruptly. A single-axis apparatus was manufactured for basic experimental study [13]. The experiments that were carried out with the apparatus have demonstrated the effectiveness of the method for generating infinite (high) stiffness against static direct disturbance. The control systems of realizing infinite stiffness can also be generalized by using a linear actuator, instead of a hybrid magnet [14].

This paper is concerned with the development of a three-degree-of-freedom (3-DoF) vibration isolation apparatus aiming

Manuscript received November 22, 2004; revised December 20, 2005. Recommended by Technical Editor R. Rajamani. This work was supported in part by a Grant-in-Aid for the Development of Innovative Technology from the Ministry of Education, Culture, Sports, Science, and Technology of Japan.

The authors are with the Department of Mechanical Engineering, Saitama University, Saitama 338-8570, Japan (e-mail: mehoque@mech.saitama-u.ac.jp; masaya@mech.saitama-u.ac.jp; ishino@mech.saitama-u.ac.jp; mizar@mech.saitama-u.ac.jp).

Digital Object Identifier 10.1109/TMECH.2006.878536

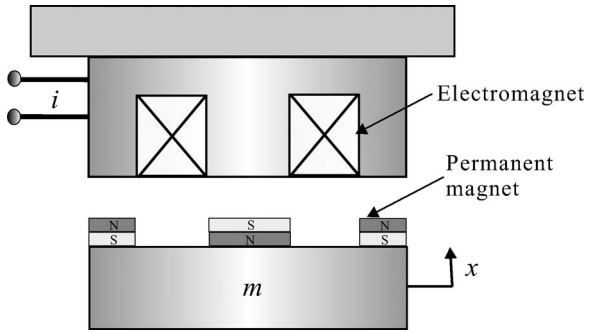

Fig. 1. Basic model of zero-power magnetic suspension system.

at industrialization, and design of controllers based on a theoretical model. 3-DoF motions of the isolation table in the vertical and rotational motions are successfully controlled by the proposed system. This paper is organized as follows. First, the concept of vibration isolation system using negative stiffness is briefly described. Second, a basic model of the developed system is analyzed and control strategies are discussed. Finally, experimental procedures and results are presented to demonstrate the efficacy of the proposed system.

II. Concept of Vibration Isolation System

A. Basic Principle

Virtually infinite (high) stiffness of a spring can be generated by connecting a normal softer spring in series with a spring that has negative stiffness and equal magnitude [8], [14]. Negative stiffness is realized by using zero-power magnetic suspension, which is discussed in Section II-B. When two springs with spring constants of k_1 and k_2 are connected in series, the total stiffness k_c is given by

$$k_c = \frac{k_1 k_2}{k_1 + k_2}. \tag{1}$$

This equation shows that the total stiffness becomes lower than that of each spring when normal springs are connected. However, if the absolute values of the springs are equal and one of the springs has negative stiffness that satisfies

$$k_1 = -k_2, \tag{2}$$

the resultant stiffness becomes infinite, i.e.,

$$|k_c| = \infty. \tag{3}$$

This research applies this principle of generating high stiffness against direct disturbance to vibration isolation systems. Moreover, if the stiffness of each spring is low enough, the system is capable to isolate ground vibrations as well.

B. Zero-Power Magnetic Suspension

1) Basic Model: A single-DoF-of-motion model for describing zero-power magnetic suspension is shown is Fig. 1. The suspended object with mass of m is assumed to move only in the vertical translational direction. The equation of motion is given by

$$m\ddot{x} = k_s x + k_i i + f_d, \tag{4}$$

where

- x is the displacement of the suspended object;
- k_s is the gap-force coefficient of the magnet;
- k_i is the current-force coefficient of the magnet;
- i is the control current; and
- f_d is the disturbance acting on the suspended object.

The transfer function representation of the dynamics described by (4) becomes

$$X(s) = \frac{1}{s^2 - a_{21}}[a_{23} I(s) + d_0 F_d(s)], \tag{5}$$

where each Laplace-transformed variable is denoted by its capital, and

$$a_{21} = \frac{k_s}{m}, \quad a_{23} = \frac{k_i}{m}, \quad d_0 = \frac{1}{m}.$$

2) Design of Control System: The zero-power control operates to accomplish

$$\lim_{t \to \infty} i(t) = 0, \tag{6}$$

for stepwise disturbances. The minimal order compensator achieving zero-power control and assigning the closed-loop poles arbitrarily can be represented as [15], [16]

$$I(s) = -\frac{s(\tilde{h}_2 s + \tilde{h}_1)}{s^2 + g_1 s + g_0} X(s), \tag{7}$$

and the characteristic polynomial of the closed-loop system is obtained as

$$t_c(s) = s^4 + g_1 s^3 + (-a_0 + g_0 + b_0 \tilde{h}_2) s^2 + (-a_0 g_1 + b_0 \tilde{h}_1) s - a_0 g_0. \tag{8}$$

Assuming that the characteristic polynomial specifying the desired location of the roots is

$$t_d(s) = (s^2 + 2\zeta_1 \omega_1 s + \omega_1^2)(s^2 + 2\zeta_2 \omega_2 s + \omega_2^2). \tag{9}$$

the coefficients of g_i's and h_i's of the controller of (7) are determined uniquely by comparing the coefficients in (8) and (9).

3) Negative Stiffness: When a constant force F_0 is applied to the suspended object, the suspended object is maintained at a position satisfying

$$0 = k_s x(\infty) + k_i i(\infty) + F_0, \tag{10}$$

in the steady states. In the zero-power control system, the coil current converges to zero, i.e.,

$$i(\infty) = 0. \tag{11}$$

Therefore,

$$x(\infty) = -\frac{F_0}{k_s}. \tag{12}$$

The negative sign appearing in the right-hand side verifies that the new equilibrium position is in the direction opposite to the applied force. It indicates that the zero-power control system behaves as if it has negative stiffness.

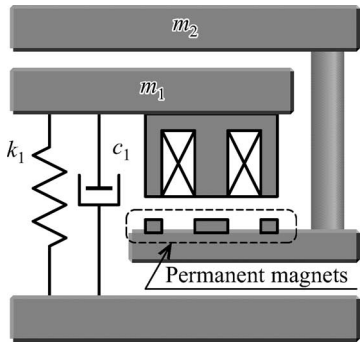

Fig. 2. Vibration isolation system using zero-power magnetic suspension.

C. Configuration of Vibration Isolation System

A schematic drawing of the proposed vibration isolation system is shown in Fig. 2 [13]. A middle table m_1 is connected to the base through a spring k_1 and a damper c_1 that work as a conventional vibration isolator. An electromagnet for zero-power magnetic suspension is fixed to the middle table. The part of an isolation table m_2 facing the electromagnet is made of soft iron material.

This system can reduce vibration transmitted from ground by setting k_1 small and, at the same time, generate infinite stiffness against direct disturbance by setting the amplitude of the negative stiffness equal to k_1.

III. Developed 3-DoF Vibration Isolator

A. Model

A 3-DoF vibration isolator has been developed so as to suppress direct disturbances, as well as ground vibrations. The schematic diagram of the manufactured vibration isolator for experimental study is shown in Fig. 3. It has a circular isolation table, a middle table, and a base. The negative stiffness is generated by three hybrid magnets, which are fixed to the middle table and suspend the isolation table. The middle table is suspended by three pairs of springs and dampers from the base. They are located at the vertices of an equilateral triangle. Each hybrid magnet is aligned with a pair of spring and damper vertically. Hence, the isolation table is suspended by three pairs of normal and negative springs so that the three modes (3-DoF motions) of the table can be controlled by the proposed mechanism. They are: one translational motion in the vertical direction (Z) and two rotational motions, roll (Θ_x) and pitch Θ_y. The coordinate system is shown in Fig. 3(b).

It is assumed that the roll and pitch angles are so small that $\cos\theta_x \cong 1, \sin\theta_x \cong \theta_x, \cos\theta_y \cong 1$, and $\sin\theta_y \cong \theta_y$, where θ_x, θ_y are the roll and pitch angles of the isolation table. The equations of motion of the isolation table can be written as

$$[M]\begin{bmatrix}\ddot{z}\\ \ddot{\theta}_x\\ \ddot{\theta}_y\end{bmatrix} = \begin{bmatrix}f_z^e\\ m_x^e\\ m_y^e\end{bmatrix} + \begin{bmatrix}f_z^d\\ m_x^d\\ m_y^d\end{bmatrix}, \tag{13}$$

and that of the middle table can be written as

$$[\bar{M}]\begin{bmatrix}\ddot{\bar{z}}\\ \ddot{\bar{\theta}}_x\\ \ddot{\bar{\theta}}_y\end{bmatrix} = -\begin{bmatrix}f_z^e\\ m_x^e\\ m_y^e\end{bmatrix} + \begin{bmatrix}f_z^p\\ m_x^p\\ m_y^p\end{bmatrix}, \tag{14}$$

where

$$[M] = \mathrm{diag}(m, J_x, J_y), \tag{15}$$

$$[\bar{M}] = \mathrm{diag}(\bar{m}, \bar{J}_x, \bar{J}_y), \tag{16}$$

m is the mass of the isolation table;
J_x is the inertial momentum of the isolation table about x-axis;
J_y is the inertial momentum of the isolation table about y-axis;
z is the displacement of the center of the isolation table;
f_z^e is the z-direction total force by the hybrid magnets;
m_x^e is the total moment about x- axis by the hybrid magnets;
m_y^e is the total moment about y- axis by the hybrid magnets;
f_z^d is the z-direction direct disturbance;
m_x^d is the direct disturbance about the x-axis;
m_y^d is the direct disturbance about the y-axis;
f_z^p is the z-direction total force by the springs and dampers;
m_x^p is the total moment about x-axis by the springs and dampers; and
m_y^p is the total moment about y-axis by the springs and dampers.

The corresponding representation of the middle table is denoted by the overbar notations.

When the hybrid magnets are located as shown by Fig. 3(c), the total force and torques are related with the forces generated by the three hybrid magnets as

$$\begin{bmatrix}f_z^e\\ m_x^e\\ m_y^e\end{bmatrix} = R_a\begin{bmatrix}f_1^e\\ f_2^e\\ f_3^e\end{bmatrix}, \tag{17}$$

and

$$R_a = \begin{bmatrix}1 & \frac{1}{\frac{\sqrt{3}r_e}{2}} & -\frac{1}{\frac{\sqrt{3}r_e}{2}}\\ 0 & \frac{r_e}{2} & \frac{r_e}{2}\\ -r_e & & \end{bmatrix}, \tag{18}$$

where

f_k^e is the attractive force of the hybrid magnet $k(k = 1, 2, 3)$ and
r_e is the distance of the hybrid magnets from the center.

The force of each magnet is approximately given by

$$f_k^e = -k_s g_k + k_i i_k \quad (k = 1, 2, 3), \tag{19}$$

where

g_k is the deviation of the gap between the electromagnet and the target on the isolation table and
i_k is the control current.

The gaps are related with the displacements as

$$\begin{bmatrix}g_1\\ g_2\\ g_3\end{bmatrix} = R_b\left(\begin{bmatrix}\bar{z}\\ \bar{\theta}_x\\ \bar{\theta}_y\end{bmatrix} - \begin{bmatrix}z\\ \theta_x\\ \theta_y\end{bmatrix}\right), \tag{20}$$

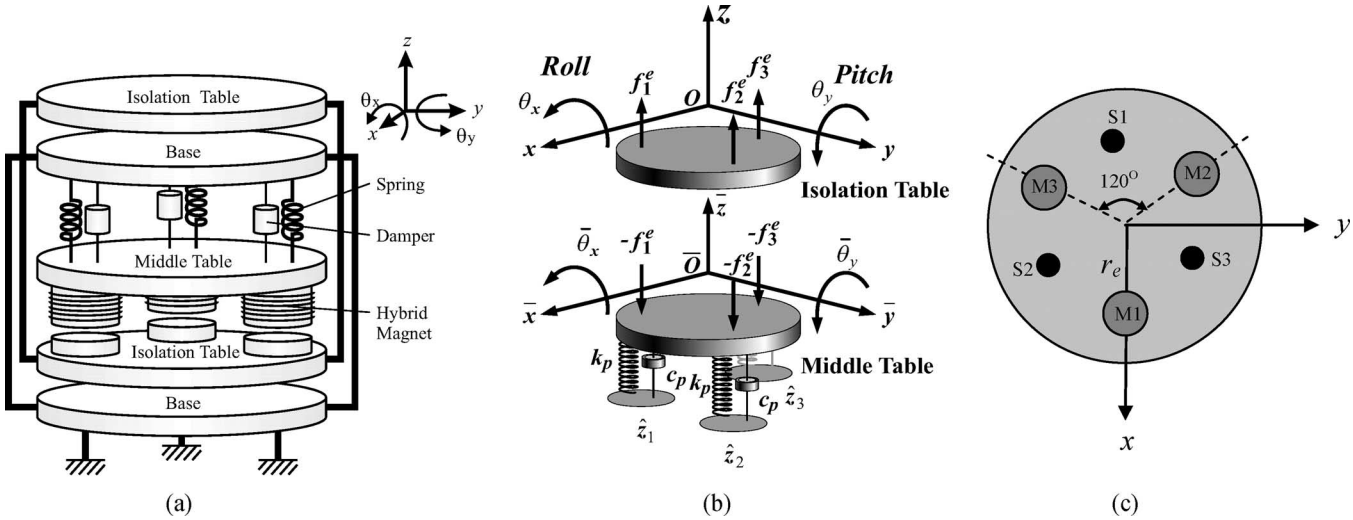

(a) (b) (c)

Fig. 3. Schematic diagram of the developed vibration isolator.

and

$$R_b = \begin{bmatrix} 1 & 0 & -r_e \\ 1 & \frac{\sqrt{3}r_e}{2} & \frac{r_e}{2} \\ 1 & -\frac{\sqrt{3}r_e}{2} & \frac{r_e}{2} \end{bmatrix}, \tag{21}$$

It is to be noted that the electromagnets on the middle table are above the targets on the isolation table at the gaps.

The total force and torques by the springs and dampers are given by

$$\begin{bmatrix} f_z^p \\ m_x^p \\ m_y^p \end{bmatrix} = R_a \begin{bmatrix} f_1^p \\ f_2^p \\ f_3^p \end{bmatrix}, \\ = R_a \left(k_p + c_p \frac{d}{dt}\right) \left(\begin{bmatrix} \hat{z}_1 \\ \hat{z}_2 \\ \hat{z}_3 \end{bmatrix} - R_b \begin{bmatrix} \bar{z} \\ \bar{\theta}_x \\ \bar{\theta}_y \end{bmatrix} \right), \tag{22}$$

where

$\hat{z}_k$ is the displacement of the base at the position k;
k_p is the stiffness of the spring; and
c_p is the damping constant of the damper.

It is found from (13) to (22) that the dynamics of the three modes can be treated separately and, in addition, each is represented in a similar form such as

$$m^\xi \ddot{\xi} = k_s^\xi (\xi - \bar{\xi}) + k_i^\xi i^\xi + w^\xi, \tag{23}$$

and

$$\bar{m}^\xi \ddot{\bar{\xi}} = -k_s^\xi (\xi - \bar{\xi}) - k_i^\xi i^\xi - (k_p^\xi + c_p^\xi \frac{d}{dt})(\bar{\xi} - \hat{\xi}). \tag{24}$$

The variables and coefficients for each mode are defined as shown in Table I.

TABLE I
VARIABLES AND COEFFICIENTS OF EACH MODE

Symbols	translation	roll	pitch
ξ	z	θ_x	θ_y
$\bar{\xi}$	$\bar{z}$	$\bar{\theta}_x$	$\bar{\theta}_y$
$\hat{\xi}$	$\frac{\hat{z}_1 + \hat{z}_2 + \hat{z}_3}{3}$	$\frac{\hat{z}_2 - \hat{z}_3}{\sqrt{3}r_e}$	$\frac{-2\hat{z}_1 + \hat{z}_2 + \hat{z}_3}{3r_e}$
m^ξ	m	J_x	J_y
$\bar{m}^\xi$	$\bar{m}$	$\bar{J}_x$	$\bar{J}_y$
k_s^ξ	$3k_s$	$\frac{3}{2}r_e^2 k_s$	$\frac{3}{2}r_e^2 k_s$
k_i^ξ	k_i	$\frac{\sqrt{3}}{2}r_e k_i$	$\frac{1}{2}r_e k_i$
i^ξ	$i_1 + i_2 + i_3$	$i_2 - i_3$	$-2i_1 + i_2 + i_3$
k_p^ξ	$3k_p$	$\frac{3}{2}r_e^2 k_p$	$\frac{3}{2}r_e^2 k_p$
c_p^ξ	$3c_p$	$\frac{3}{2}r_e^2 c_p$	$\frac{3}{2}r_e^2 c_p$
w^ξ	f_z^d	m_x^d	m_y^d

B. Control Strategy

The developed vibration isolation system is a three-channel multiple-input multiple output system. Since the number of actuators for the zero-power control and the number of modes are equal, two control strategies are possible. They are local control [15] and mode control [16]. In the former, the coil current of each magnet is controlled on the basis of local information at the corresponding position as shown in Fig. 4(a). In the latter, a controller is designed for each of the modes (Z, Θ_x, and Θ_y) as shown in Fig. 4(b). Sensors 1, 2, and 3 are the displacement signals of the table measured from the corresponding hybrid magnets, respectively. In the case of mode-based control, the displacement signal of three modes ($X_z, X_{\theta x}$, and $X_{\theta y}$) are calculated from the sensor signals. Again the control currents (i_1, i_2, i_3) for three hybrid magnets are calculated from

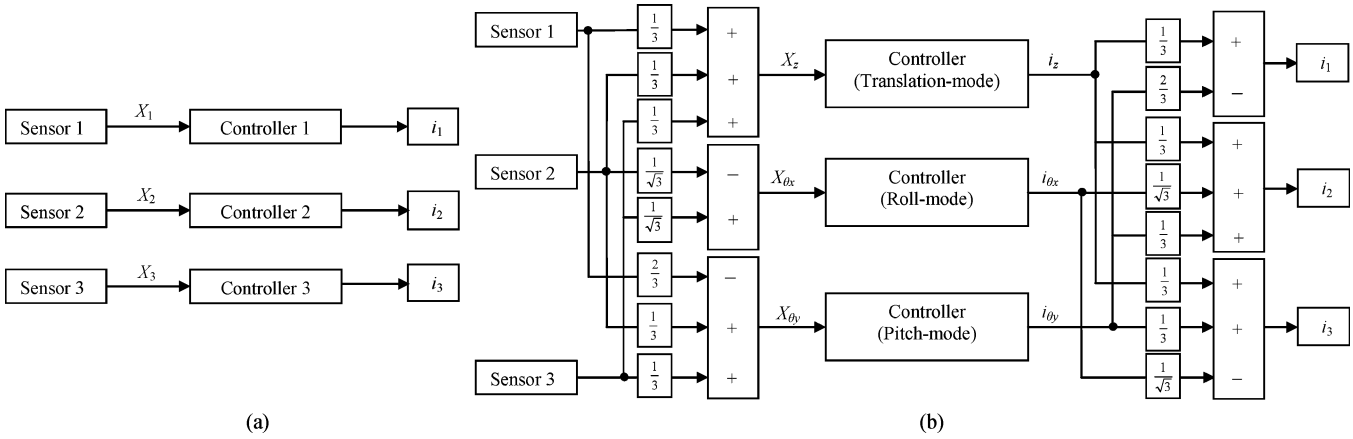

Fig. 4. Block diagram of the proposed controllers. (a) Local control. (b) Mode control.

the outputs ($i_z, i_{\theta x}$, and $i_{\theta y}$) of the zero-power controllers. The zero-power controller of each channel is designed to have such dynamics as (7)

$$I_\xi(s) = -\frac{s(\tilde{h}_2 s + \tilde{h}_1)}{s^2 + g_1 s + g_0}\xi(s) = -sc_2^\xi(s)\xi(s). \tag{25}$$

C. Response to Direct Disturbance

It is assumed for simplicity that the initial values are zero. Equations(23)–(25) yield

$$\Xi(s) = \frac{(c_p^\xi s + k_p^\xi)(k_i^\xi c_2^\xi(s)s - k_s^\xi)}{t_c(s)}\hat{\Xi}(s) + \frac{t_1(s) + k_i^\xi c_2^\xi(s)s - k_s^\xi}{t_c(s)}W^\xi(s), \tag{26}$$

$$\bar{\Xi}(s) = \frac{(c_p^\xi s + k_p^\xi)t_2(s)}{t_c(s)}\hat{\Xi}(s) + \frac{k_i^\xi c_2^\xi(s)s - k_s^\xi}{t_c(s)}W^\xi(s), \tag{27}$$

$$t_1(s) = \bar{m}^\xi s^2 + c_p^\xi s + k_p^\xi, \tag{28}$$

$$t_2(s) = m^\xi s^2 + k_i^\xi c_2^\xi(s)s - k_s^\xi, \tag{29}$$

$$t_c(s) = t_1(s)t_2(s) + m^\xi s^2(k_i^\xi c_2^\xi(s)s - k_s^\xi). \tag{30}$$

To estimate the stiffness for direct disturbance, the direct disturbance W^ξ is assumed to be stepwise, i.e.,

$$W^\xi = \frac{F_0}{s} \quad (F_0 : \text{ const}). \tag{31}$$

When the vibration of the floor is neglected, the steady-state displacement of the table is obtained as

$$\frac{\xi(\infty)}{F_0} = \lim_{s\to 0}\frac{m^\xi s^2 + (c_p^\xi + k_i^\xi c_2^\xi(s))s + k_p^\xi - k_s^\xi}{t_c(s)} \tag{32}$$

$$= \frac{1}{k_p^\xi} - \frac{1}{k_s^\xi} = 0 \quad (\text{when } k_p^\xi = k_s^\xi). \tag{33}$$

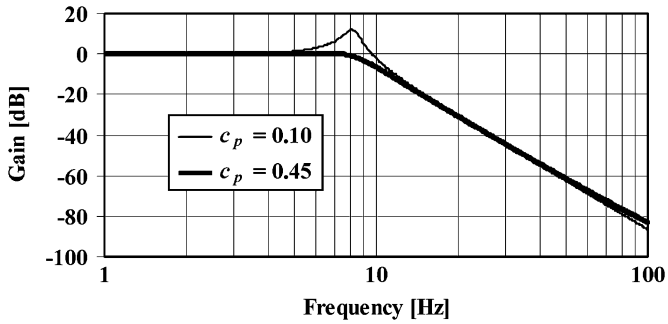

Fig. 5. Analytical displacement transfer function (transmissibility) of the isolator from floor.

Since $k_p^\xi = k_s^\xi$ is satisfied in three modes, therefore, the suspension system between the isolation table and the floor has infinite stiffness.

D. Response to Floor Vibrations

When the direct disturbances are assumed to be neglected, the transmissibility of the isolator from the floor during floor excitation along vertical translation mode (Z), can be written from (26) as

$$\frac{\Xi(s)}{\hat{\Xi}(s)} = \frac{(3c_p s + 3k_p)(k_i c_2^z(s)s - 3k_s)}{t_c(s)}. \tag{34}$$

The parameters of (34) are chosen as, $k_i = 57.2$ N/A, $|3k_p| = |3k_s| = 59.5$ N/mm and, the closed-loop poles for c_2^z are selected by putting $\omega(= \omega_1 = \omega_2) = 2\pi \times 4$ [1/s] and $\zeta(= \zeta_1 = \zeta_2) = 1.0$ in (9). Fig. 5 shows the analytical displacement transfer function (transmissibility) of the isolator. It is found that a suitable damping (c_p) between base to middle table could suppress the amplitude of resonance effectively and the vibration isolation performance is not worsened during floor vibrations.

IV. Experiment

A. Experimental Setup

The photograph of the developed vibration isolation system is shown in Fig. 6. Each hybrid magnet for zero-power

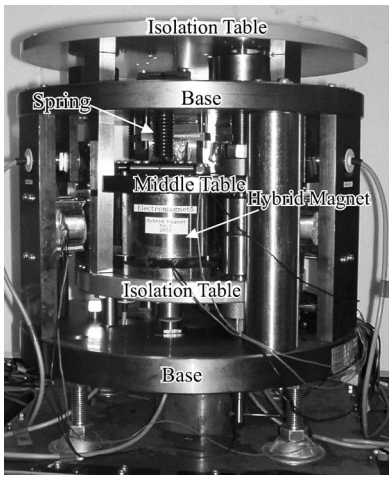

Fig. 6. Photograph of the developed isolator.

magnetic suspension consisted of a disk-shaped permanent magnet (30 mm $\times$ 10 mm) and a 2500-turn electromagnet. The permanent magnet was made of NdFeB materials. The stiffness of each normal spring was 20 N/mm. As a damper parallel with the normal spring, an actively controlled electromagnet was used. It enabled the stiffness and damping characteristics of the normal springs to be adjusted flexibly.

The height, diameter, and mass of the apparatus were 400 mm, 440 mm, and 150 kg, respectively. The isolation and middle tables weighed 22 kg and 23 kg, respectively. The radial motions of the isolation table were confined by the other three electromagnets while those of the middle table were constrained by the three springs for positive stiffness.

The relative displacements of the middle table to the base and those of the isolation table to the middle table were detected by six eddy-current gap sensors provided by Baumer electric. The radial displacements of the isolation table were measured by another three gap sensors, and the radial motions of the table were actively controlled. Designed control algorithms were implemented with a digital controller DS1103 supplied by dSPACE. The sampling rate was 10 kHz.

B. Experimental Results

The experiment was carried out with the controllers based on local control and mode control. Furthermore, the system performances were evaluated by measuring the static and dynamic response of the isolation table to direct disturbances and the transmissibility characteristics of the isolation table from the base during floor excitations.

1) Response to Direct Disturbances: First, the static response of the isolation table to direct disturbance using local control and mode control were measured for three modes. Direct static loads were added to the center of the table for vertical translational mode and on the y- and x-axes (150-mm apart from center) for roll and pitch modes, respectively. Fig. 7 shows the results using local control. It is found that displacement of the

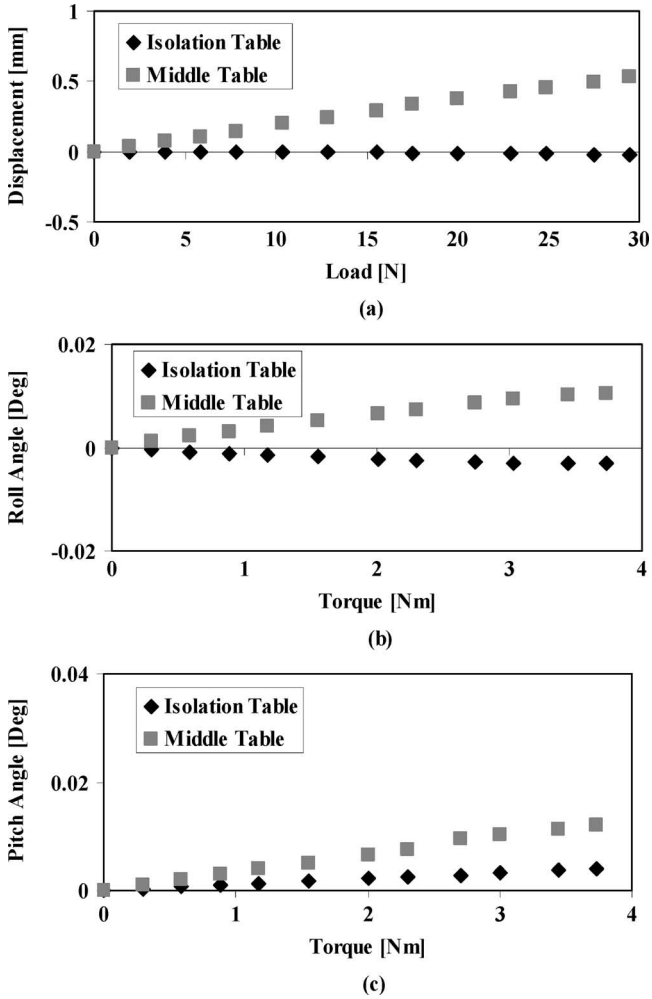

Fig. 7. Static response of the local control isolator to direct disturbance. (a) Translation (Z). (b) Roll. (c) Pitch.

isolator along vertical translational mode and the rotational angle of the isolator along roll and pitch axis were small compared to that of the middle table. Fig. 8 shows the static characteristic of the isolator using mode control. It is observed from different modes that the table was maintained almost at the same position, while the position of the middle table changed proportional to the load. It is also found that the stiffness of the isolator using mode control was 1.4 times in the vertical translation mode, 11.8 times in the roll mode, and 11 times in the pitch mode, more than that of using local control. It is obvious that suppressing direct disturbances along rotational modes was weaker in the case of using local control. It can be noted that positive stiffness along rolling axis could be adjusted to make the rolling stiffness of the isolator stronger. But, in that case, the other two stiffnesses would be weaker. The same was true for pitch axis.

Next, the dynamic responses of the isolation table were measured. In this case, the table was excited by two voice coil motors along the z-axis. Fig. 9 shows the frequency response of the isolator in the vertical translational (Z) mode when local

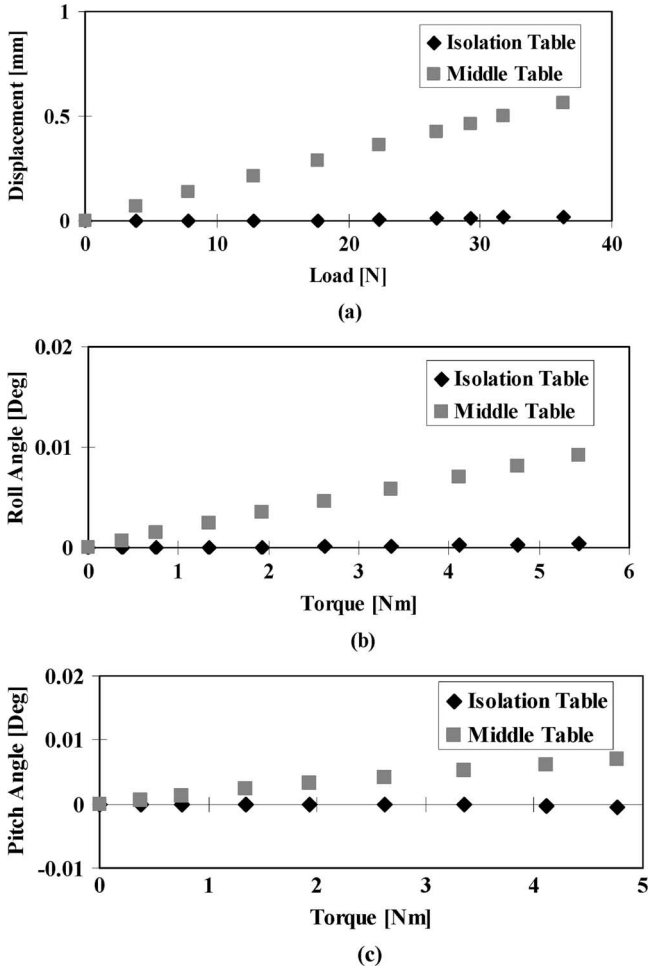

Fig. 8. Static response of the mode control isolator to direct disturbance. (a) Translation (Z). (b) Roll. (c) Pitch.

control was used. It is seen from the figure that the displacement of the isolation table at low frequency (0.015 Hz) was much lower (-28 dB) than that of the middle table. Fig. 10 shows the results of using mode control. In this experiment, the closed-loop poles of the controller were assigned by varying the design frequency $(\omega_1 = \omega_2 = \omega)$ from $2\pi \times 3$ [1/s] to $2\pi \times 6$ [1/s], while the damping ratio $(\zeta_1 = \zeta_2 = \zeta)$ was fixed to 1.0. It was found from Fig. 10(a) that the displacement of the isolation table (-48 dB) is much lower than the middle table (-37 dB) at 0.15 Hz. Fig. 10(b) and (c) shows that the displacement of the isolation table is further reduced (-69 dB at $\omega = 2\pi \times 6$ [1/s]) by selecting higher closed-loop poles.

2) Response to Floor Vibrations: In the second experiment, the absolute transmissibility of the isolator $(z/\hat{z})$ from the floor was measured at the center of the table by exciting the base of the apparatus vertically by a pneumatic actuator. Fig. 11 shows the transmissibility characteristics of the isolator using local control. The experiments were carried out by changing the damping coefficients (c_p) of the damper electromagnet located between the base and the middle table. The result shows

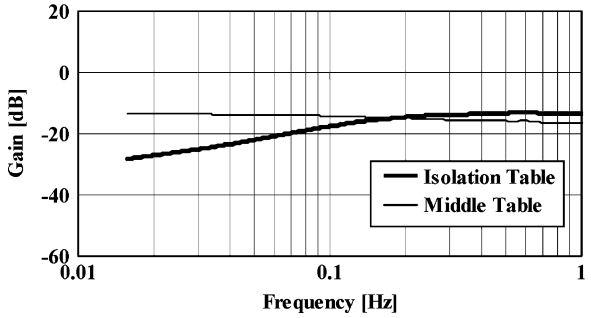

Fig. 9. Frequency response of the local control isolator to direct disturbances along Z axis.

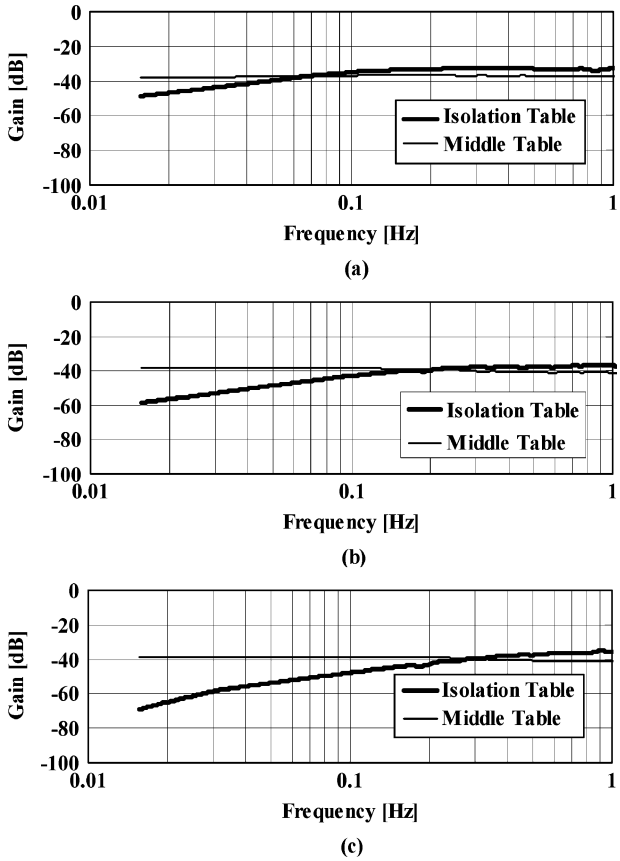

Fig. 10. Frequency responses of the mode control isolator to direct disturbances along Z axis. (a) $\omega = 2\pi \times 3$ [1/s]. (b) $\omega = 2\pi \times 4.5$ [1/s]. (c) $\omega = 2\pi \times 6$ [1/s].

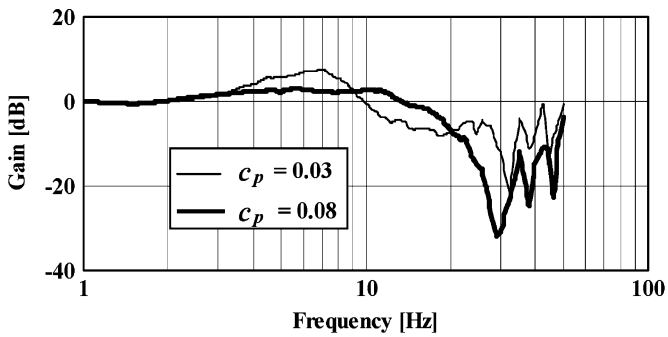

Fig. 11. Absolute transmissibility of the local control isolator from the floor during floor excitation.

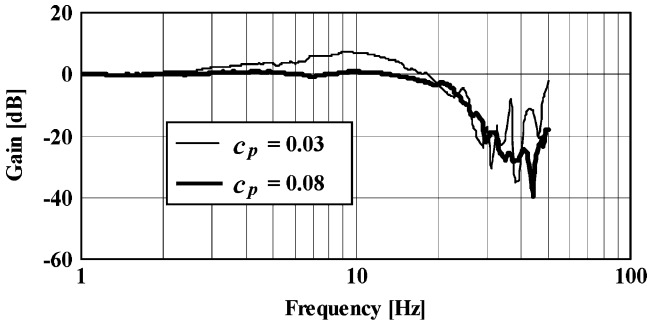

Fig. 12. Absolute transmissibility of the mode control isolator from the floor during floor excitation.

that increasing the damping coefficient could improve the vibration isolation performances. The isolation performance was further improved when mode control was used, as shown in Fig. 12. The closed-loop poles of the zero-power controller for Z-mode were selected as $\omega(=\omega_1=\omega_2)=2\pi\times 3$ [1/s] and $\zeta(=\zeta_1=\zeta_2)=1.4$. It is obvious that the resonance peak was damped down in case of higher damping. It agreed with the theoretical transmissibility calculated from the model (Fig. 5), except that the resonance frequency of the middle table and that of the pneumatic vibration table affected the experimental results. It is revealed that ground vibration isolation performance, nonetheless, was not worsened in the case of generating high stiffness to suppress the effect of direct disturbances.

V. Conclusion

An active 3-DoF vibration isolation system using zero-power controller was developed and two control strategies were proposed. The experimental results revealed that the mode-based controller was better for multi-DoF system, while local control could better be applicable for single-DoF and unit-based system. The developed vibration isolator using eddy-current gap sensor realized high stiffness to static and low-frequency direct disturbances and showed good capability to suppress direct disturbance. It is obvious from the transmissibility characteristic that the system could isolate ground vibration in vertical direction effectively. The system performances, both for suppressing the effect of direct disturbances and isolating ground vibrations, could further be improved by assigning the proper closed-loop pole of the zero-power controllers and selecting suitable damping between the base to the middle table. It is hoped that the controller has a possibility to be used in the wide application range. The developed isolator performed very well in the analytical and experimental phase and, with further development, it could materialize the basis of an industrially and commercially feasible, adaptable, and compliant isolator for hi-tech systems.

Acknowledgment

The authors would like to thank H. Suzuki for his contributions to this project regarding the design and fabrication of the apparatus.

References

[1] S. T. Ho, H. Matsuhisa, and Y. Honda, "Passive vibration suppression of beam with piezoelectric elements," *JSME Int. J., Ser. C*, vol. 43, no. 3, pp. 740–747, 2000.

[2] E. I. Rivin, *Passive Vibration Isolation*. New York: ASME, 2003.

[3] M. Yasuda and M. Ikeda, "Double-active control of microvibration isolation systems to improve performances (application of two-degree-of-freedom control)," *Trans. Jpn. Soc. Mech. Eng.*, vol. 59, no. 562, pp. 1694–1701, 1993.

[4] H. Yoshioka, Y. Takahashi, K. Katayama, T. Imazawa, and N. Murai, "An active microvibration isolation system for hi-tech manufacturing facilities," *ASME J. Vib. Acoust.*, vol. 123, pp. 269–275, 2001.

[5] M. Yasuda, T. Osaka, and M. Ikeda, "Feedforward control of a vibration isolation system for disturbance suppression," in *Proc. 35th IEEE Conf. Decision Contr.*, Kobe, Japan, 1996, pp. 1229–1233.

[6] K. Watanabe, S. Hara, Y. Kanemitsu, T. Haga, K. Yano, T. Mizuno, and R. Katamura, "Combination of H^{∞} and PI control for an electromagnetically levitated vibration isolation system," in *Proc. 35th IEEE Conf. Decision Contr.*, Kobe, Japan, 1996, pp. 1223–1228.

[7] D. L. Trumper and T. Sato, "A vibration isolation platform," *Mechatron.*, vol. 12, pp. 281–294, 2002.

[8] T. Mizuno, "Proposal of a vibration isolation system using zero-power magnetic suspension," in *Proc. Asia-Pac. Vib. Conf.*, 2001, vol. 2, pp. 423–427.

[9] A. V. Sabnis, J. B. Dendi, and F. M. Schmitt, "A magnetically suspended large momentum wheel," *J. Spacecraft*, vol. 12, pp. 420–427, 1975.

[10] M. Morishita, T. Azukizawa, S. Kanda, N. Tamura, and T. Yokoyama, "A new Maglev system for magnetically levitated carrier system," *IEEE Trans. Veh. Technol.*, vol. 38, no. 4, pp. 230–236, 1989.

[11] D. L. Platus, "Negative-stiffness-mechanism vibration isolation systems," in *Proc. SPIE Conf. Vib. Contr. Microelectron Opt. Metrol.*, 1991, vol. 1619, pp. 44–54.

[12] ——, "Negative-stiffness-mechanism vibration isolation systems," in *Proc. SPIE Conf. Curr. Dev. Vib. Contr. Optomech. Syst.*, 1999, vol. 3786, pp. 98–105.

[13] T. Mizuno, "Vibration isolation system using zero-power magnetic suspension," presented at the Preprints of the 15th World Congress IFAC, 2002, Paper 955.

[14] T. Mizuno, T. Toumiya, and M. Takasaki, "Vibration isolation system using negative stiffness," *JSME Int. J., Ser. C*, vol. 46, no. 3, pp. 807–812, 2003.

[15] T. Mizuno, M. Takasaki, H. Suzuki, and Y. Ishino, "Development of a three-axis active vibration isolation system using zero-power magnetic suspension," in *Proc. 42nd IEEE Conf. Decision Contr.*, Hawaii, Dec. 2003, pp. 4493–4498.

[16] M. E. Hoque, M. Takasaki, Y. Ishino, and T. Mizuno, "Design of a mode-based controller for 3-DoF vibration isolation system," in *Proc. 2004 IEEE Conf. Robot. Autom. Mechatron.*, Singapore, pp. 478–483.

Md. Emdadul Hoque (S'06) received the B.Sc. and M.Eng. degrees in mechanical engineering from Rajshahi University of Engineering and Technology, Rajshahi, Bangladesh, and Nanyang Technological University, Singapore, in 1996 and 2003, respectively. Currently, he is working toward the Ph.D. degree in the Department of Mechanical Engineering, Saitama University, Saitama, Japan.

Since 1996, he has been with Rajshahi University of Engineering and Technology. His current research interests include active control, magnetic levitation, zero-power control, and vibration isolation.

Mr. Hoque is a member of the American Society of Mechanical Engineers, the Society of Instrument and Control Engineers, Japan, and Institution of Engineers, Bangladesh.

Masaya Takasaki (A'05) received the B.E., M.E., and Ph.D. degrees from the University of Tokyo, Tokyo, Japan, in 1996, 1998, and 2001, respectively.

Since 2001, he has been a Research Associate in the Department of Mechanical Engineering at Saitama University, Saitama, Japan. His current research interests include magnetic suspension, ultrasonic application for mechatronics, surface acoustic wave utilization, and tactile display.

Dr. Takasaki is a member of the Japan Society of Mechanical Engineers, the Society of Instrument and Control Engineers, the Institute of Electrical Engineers of Japan, the Japan Society for Precision Engineering, the Japan Society of Applied Electromagnetics and Mechanics, and the Virtual Reality Society of Japan.

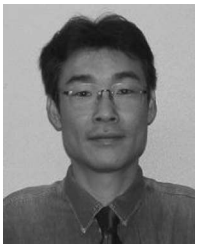

Yuji Ishino graduated from the University of Tsukuba, Tsukuba, Japan, in 1988.

Since 1988, he has been working as a Technician with the Department of Mechanical Engineering, Saitama University, Saitama, Japan. His current research interests include magnetic suspension, vibration isolation, and mass measurement under microgravity conditions.

Takeshi Mizuno (M'00) graduated from the Department of Mathematical Engineering and Instrumentation Physics, University of Tokyo, Tokyo, Japan, in 1978. He received the M.Eng. and Ph.D. degrees from the University of Tokyo, in 1980 and 1985, respectively.

From 1980 to 1985, he was a Research Associate at the Institute of Industrial Science, University of Tokyo. During 1985–1988, he was an Assistant Professor at the Polytech University, Japan. From 1988 to 2000, he was an Associate Professor, and since 2000, he has been a Professor in the Department of Mechanical Engineering, Saitama University, Saitama, Japan. From 1990 to 1991, he worked at the Swiss Federal Institute of Technology (Eidgenössische Technische Hochschule Zürich), Zurich, Switzerland. His current reserach interests include magnetic bearings, magnetic and electric suspension technology, vibration control, mechatronics, and application of dynamic vibration absorber.

Prof. Mizuno is a member of the American Society of Mechanical Engineers, the Society of Instrument and Control Engineers, the Japan Society of Mechanical Engineering, the Institute of Systems, Control, and Information Engineers, and the Japan Society for Precision Engineering. He is the recipient of numerous awards for paper and research performances.